

# Experimental Studies on the Combustion Characteristics of Multisource Organic Solid Waste for Collaborative Disposal Using Municipal Solid Waste Incinerators

Xiaohui Zhuo, Mi Li, Qiang Cheng, and Zixue Luo\*



Cite This: *ACS Omega* 2024, 9, 2911–2919



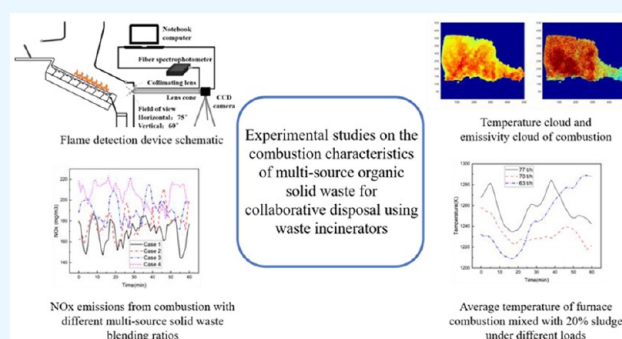
Read Online

ACCESS |

Metrics & More

Article Recommendations

**ABSTRACT:** This study investigated the evolution of furnace conditions during the heat conversion process of multisource organic solid waste. To achieve this, combustion tests involving different sludge mixing ratios, variable load operation, and multisource organic solid waste collaborative disposal were performed on a 750 t/d new municipal solid waste incineration grate furnace. The test results revealed that as the sludge mixing ratios increased from 0 to 10 and 20%, the temperature level in the furnace decreased and the fuel-type NO<sub>x</sub> emission increased. Moreover, the sludge featured poor combustion stability under low-load conditions owing to fluctuations in its calorific value and moisture content. Field tests of multisource organic solid waste revealed that after mixing waste cloth strips and papermaking waste, the temperature level in the furnace increased. Additionally, the emissivity distribution was positively correlated with the furnace flame temperature distribution, and NO<sub>x</sub> emissions also increased. The overall results indicated the feasibility of controlling the mixing rate of different organic solid wastes in the municipal solid waste incinerator within a reasonable range for cooperative incineration.



## 1. INTRODUCTION

The development of China's economy and society has led to a rapid increase in the output of organic solid waste from residential and industrial sources.<sup>1–3</sup> Traditional landfill and stacking treatment methods require a large amount of land resources and pose threats to both the ecological environment and human health owing to the presence of toxic substances such as heavy metals contained in solid waste.<sup>4–9</sup> Moreover, organic solid waste contains a high organic matter content, and its resource-based disposal to alleviate environmental pollution has become a vital treatment method. After incinerating organic solid waste, its volume is reduced by 90%, its weight is reduced by 80%, a large number of harmful substances are dissolved during the incineration process, and the waste heat energy generated through incineration is used for power generation and heat supply.<sup>10–13</sup> Therefore, incineration is the most suitable waste treatment method.<sup>14–16</sup>

Currently, the incineration treatment industry mainly focuses on municipal solid waste (MSW) incineration. According to the 2022 National Statistical Yearbook, China has 583 municipal solid waste incineration power plants, with a daily incineration treatment capacity of 740,000 tons.<sup>17</sup> However, the separate incineration of organic solid wastes such as sludge and industrial solid waste (hazardous waste)

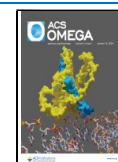
poses a high technical challenge. Moreover, the operation results in the production of flue gas, leading to higher operating costs and significant one-time investment costs.<sup>18–22</sup> Chen et al.<sup>23,24</sup> characterized coal gasification fine ash with NaOH/HCl hydrothermal treatment and low-temperature alkali fusion operation to realize the resource coal gasification fine ash. Chen Wei<sup>25</sup> investigated a municipal solid waste incineration grate furnace with a capacity of 750 t/d and analyzed the gas–solid combustion with different sludge mixing ratios through numerical simulation methods. The results revealed that with increasing mixing ratio, the temperature of the furnace combustion area gradually decreased and the NO generation decreased. A sludge mixing ratio of 10% displayed a minimal effect on the combustion process. Wang<sup>26</sup> conducted experimental research on the collaborative incineration of municipal solid waste and industrial solid waste using a pilot test bench and selected

**Received:** October 24, 2023

**Revised:** December 15, 2023

**Accepted:** December 15, 2023

**Published:** January 3, 2024



textile solid waste and papermaking solid waste as representative industrial solid wastes. The test results revealed that the mixing of textile and papermaking wastes featured no significant effect on the grate temperature and exhaust gas temperature. Additionally, the flue gas pollutants featured low emission levels, confirming the feasibility of mixing and utilizing textile solid waste and papermaking solid waste. Chen et al.<sup>27</sup> investigated the change in the heavy metal content of fly ash before and after mixing municipal solid waste with 2% sludge and found that the heavy metal content in fly ash increased after the addition of sludge.

The use of municipal solid waste incinerators to manage the disposal of multisource organic solid waste meets the actual demand for reducing, recycling, and safely processing solid waste generated from both domestic and industrial sources. Therefore, this study mainly focused on the experiments of different sludge mixing ratios, operations under variable load conditions after mixing sludge, and the mixing of multisource organic solid waste in municipal solid waste incinerators. In this study, a CCD camera and a spectrometer were used to detect the combustion conditions in the furnace, to explore the variations in combustion conditions in the furnace. This study provides guidance for operating and regulating the collaborative disposal of multisource organic solid waste in municipal solid waste incinerators.

## 2. TEST SETUP

**2.1. Municipal Solid Waste Incinerators.** The municipal solid waste incinerator (SGF-V) used in this experiment featured a processing capacity of 750 tons/day, a grate length of 9820 mm, a width of 14,400 mm, and a grate operating speed of 9820 mm/h. The field test involved collecting radiation intensity data from six different viewing holes of the incinerator to comprehensively analyze the temperature distribution and radiation characteristics in the incinerator under various working conditions (Figure 1).

Among these viewing holes, the four measurement ports (named #2, #3, #4, and #5) were evenly spaced on the back wall, at an elevation of 15,295 mm. The other two measuring

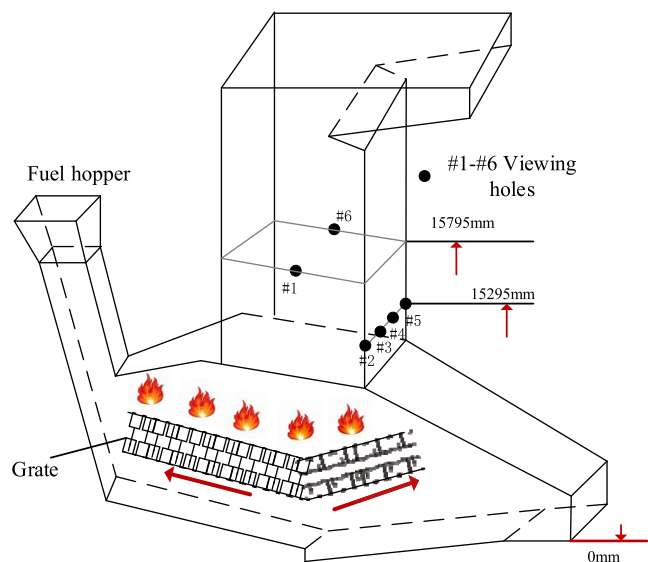


**Figure 1.** Municipal solid waste incinerator and test measurement point layout drawing.

ports were distributed on the left and right walls (#6 and #1) at an elevation of 15,795 mm.

Based on this incinerator, a numerical simulation model was established to simulate the process of waste coincineration treatment using the coupled method of FLIC and Fluent. Figure 2 shows the incinerator measurement point distribution; a total of nine temperature measurement points (numbered 1–9) are arranged in the first flue of the grate furnace.

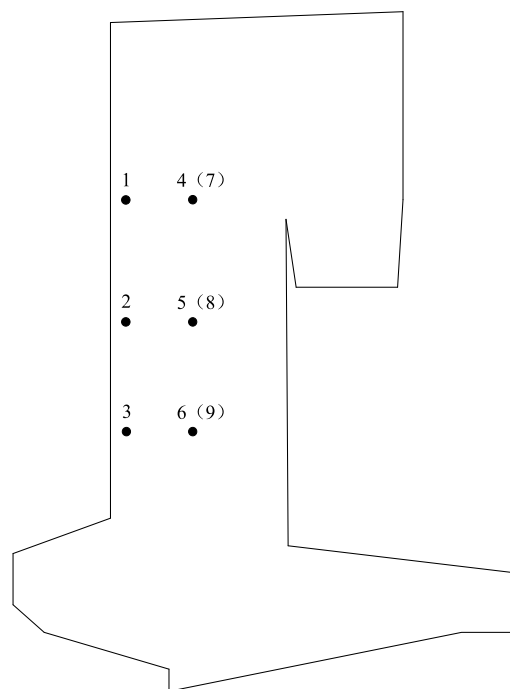


**Figure 2.** Measurement point layout drawing.

Comparing the simulation data of pure municipal solid waste combustion with the actual operation monitoring data on-site, the data error of the simulation results is within 5% (Table 1), which can better reflect the actual combustion process in the furnace,<sup>28</sup> and furthermore, we carried out the field test work.

**2.2. Test and Testing Equipment.** Figure 3 shows the test and detection device setup. A CCD camera and a spectrometer were set up directly opposite the furnace at the flame-viewing holes, and a high-temperature mirror rod was equipped to obtain a larger field of view. The CCD camera

**Table 1.** Comparison of Measured and Simulated Temperatures at the First Flue Measurement Point

measurement point	measured temperature (K)	simulated temperature (K)	error (%)
1	1265.09	1324.359	4.68
2	1303.99	1341.882	2.91
3	1320.65	1355.806	2.66
4	1267.82	1320.287	4.14
5	1272.92	1334.998	4.88
6	1289.8	1342.229	4.06
7	1285.18	1316.216	2.41
8	1347.08	1331.309	−1.17
9	1365.66	1339.927	−1.88

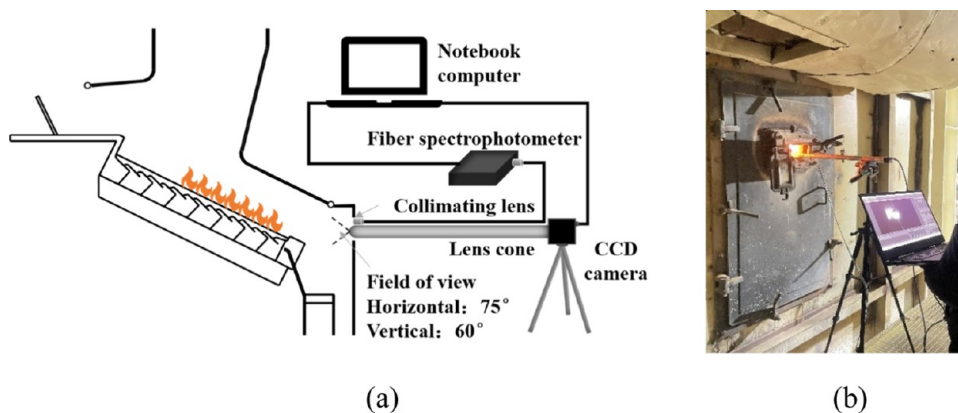


Figure 3. Flame detection device: (a) schematic and (b) field testing.

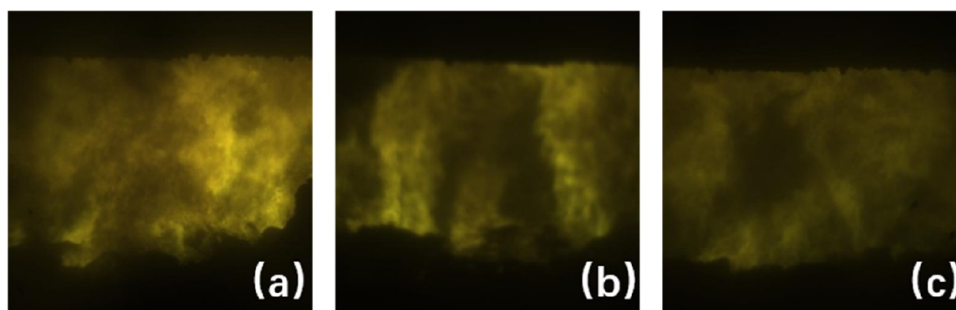


Figure 4. Original image of the flame: (a) 0% sludge; (b) 10% sludge; and (c) 20% sludge.

model used in the test was MER2-231-41U3M/C. Additionally, the spectrometer model used was AvaSpec-ULS2048CL-EVO with a spectral wavelength range of 200–1100 nm and a spectral resolution of 0.6 nm. Before conducting the test, the calibration of the CCD camera and the spectrometer was performed using a blackbody furnace to establish a relationship between the response value of the equipment and the absolute radiation intensity of the actual detection object. Figure 4 shows the original image of the flame at different sludge mixing ratios.

### 3. MEASUREMENT PRINCIPLE

The radiation intensity of an object with wavelength  $\lambda$ , temperature  $T$ , and blackness  $\varepsilon(\lambda)$  was calculated according to Planck's law

$$I(\lambda, T) = \varepsilon(\lambda) \frac{2\pi hc^2}{\lambda^5 (e^{hc/\lambda kT} - 1)} \quad (1)$$

where  $h$  is Planck's constant;  $c$  is the speed of light; and  $k$  is the Boltzmann constant. For radiation objects with temperatures in the range of 800–2000 K and wavelengths in the range of 300–1000 nm,  $hc/\lambda kT \gg 1$ , the Wien displacement law was used instead of Planck's law

$$I(\lambda, T) = \varepsilon(\lambda) I_b(\lambda, T) \quad (2)$$

where  $I_b(\lambda, T)$  is the intensity of the monochromatic blackbody radiation of the radiating object.

According to the gray judgment principle of the two-color method, the spectral detection system was used to obtain the two monochromatic radiation intensities  $I(\lambda, T)$  and  $I(\lambda + \Delta\lambda, T)$  emitted by the radiation object from the same direction. The intensities were classified into two to obtain

$$\frac{I(\lambda, T)}{I(\lambda + \Delta\lambda, T)} = \left( \frac{\varepsilon_\lambda}{\varepsilon_{\lambda + \Delta\lambda}} \right) \frac{(\lambda + \Delta\lambda)^5}{\lambda^5} \exp \left[ -\frac{C_2}{T} \left( \frac{1}{\lambda} - \frac{1}{\lambda + \Delta\lambda} \right) \right] \quad (3)$$

where  $\varepsilon_\lambda$  represents the blackness of the radiation object at wavelength  $\lambda$  and  $\varepsilon_{\lambda + \Delta\lambda}$  denotes the blackness of the object at wavelength  $\lambda + \Delta\lambda$ . At a smaller  $\Delta\lambda$ ,  $\varepsilon_\lambda/\varepsilon_{\lambda + \Delta\lambda} \approx 1$ ; the temperature distribution can be calculated from the corresponding monochromatic radiation intensity  $I(\lambda, T)$  and  $I(\lambda + \Delta\lambda, T)$  ratio of  $\lambda$  and  $\lambda + \Delta\lambda$

$$T = -C_2 \left( \frac{1}{\lambda} - \frac{1}{\lambda + \Delta\lambda} \right) / \ln \left[ \frac{I(\lambda, T)}{I(\lambda + \Delta\lambda, T)} \frac{\lambda^5}{(\lambda + \Delta\lambda)^5} \right] \quad (4)$$

After obtaining  $T$ , the  $\varepsilon_\lambda$  distribution can be calculated through the comparison of the detected radiation intensity with the blackbody intensity at the same  $T$

$$\varepsilon(\lambda) = \frac{I(\lambda, T)}{I_b(\lambda, T)} \quad (5)$$

If the calculated  $\varepsilon(\lambda)$  varies with wavelength, the radiation object does not satisfy the gray hypothesis. The magnitude of fluctuations in  $\varepsilon(\lambda)$  and  $T$  was assessed using relative mean square deviation. The average temperatures,  $T_a$  and  $\varepsilon_a$ , can be obtained using eq 6

$$T_a = \frac{1}{m} \sum_{i=1}^m T_i, \quad \varepsilon_a = \frac{1}{m} \sum_{i=1}^m \varepsilon_i \quad (6)$$

Table 2. Proximate and Ultimate Analyses of Multisource Organic Solid Waste Introduced into the Furnace

	proximate analysis				ultimate analysis					
	M <sub>ar</sub> (%)	FC <sub>ar</sub> (%)	V <sub>ar</sub> (%)	A <sub>ar</sub> (%)	C <sub>ar</sub> (%)	H <sub>ar</sub> (%)	O <sub>ar</sub> (%)	N <sub>ar</sub> (%)	S <sub>ar</sub> (%)	Q <sub>d</sub> (kJ/kg)
MSW	55.48	11.25	24.91	8.36	60.26	6.83	29.12	2.4	0.47	7200
sludge	45	0.05	21.24	33.71	46.59	7.75	39.27	6.39		4748
cloth strips	10.82	11.5	76.66	1.02	53.88	6.3	38.34	1.26	0.11	17,500
papermaking waste	59	1.19	38.28	1.53	63.03	5.6	26.3	5.07		10,199

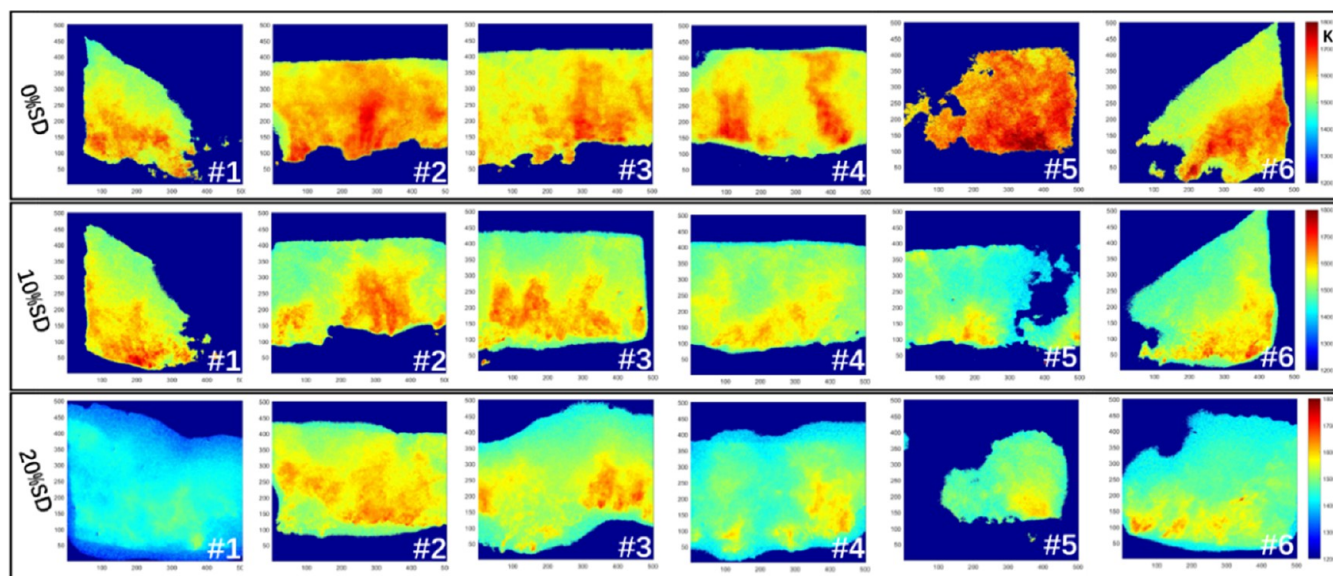


Figure 5. Temperature cloud diagram of furnace combustion under different sludge mixing ratios.

where  $T_i$  is the calculated temperature for a set of wavelengths;  $m$  is the number of wavelengths calculated; and  $\varepsilon_i$  is the calculated blackness distribution.

The relative mean square deviation of  $\sigma_T$  and  $\sigma_\varepsilon$  is calculated using eqs 7 and 8, respectively. Additionally, if  $\sigma_\varepsilon$  is <5%, the radiation object can meet the gray body hypothesis in the calculated wavelength band.

$$\sigma_T = \sqrt{\frac{1}{m-1} \sum_{i=1}^m (T_i - T_a)^2 / T_a} \quad (7)$$

$$\sigma_\varepsilon = \sqrt{\frac{1}{m-1} \sum_{i=1}^m (\varepsilon_i - \varepsilon_a)^2 / \varepsilon_a} \quad (8)$$

After using the above-mentioned method to evaluate the gray body hypothesis, for the flame image acquisition system, if the wavelengths at the corresponding centers of CCD cameras R and G meet the gray body hypothesis, the temperature calculation can be performed according to the principle of the two-color method.

$$T = -C_2 \left( \frac{1}{\lambda_R} - \frac{1}{\lambda_G} \right) / \ln \left( \frac{I_r(\lambda_r, T) \lambda_r^5 \varepsilon_g}{I_g(\lambda_g, T) \lambda_g^5 \varepsilon_r} \right) \quad (9)$$

#### 4. RESULTS AND DISCUSSION

According to the actual condition on-site, a part of the sludge has been mixed in the incinerator for long-term collaborative treatment. Sludge is characterized by its high moisture content, low calorific value of combustion, high ash content, and high heavy metal content.<sup>29–31</sup> However, the actual blending

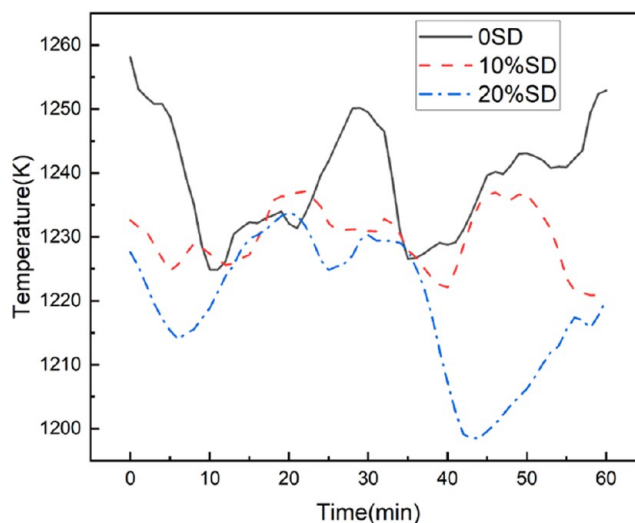
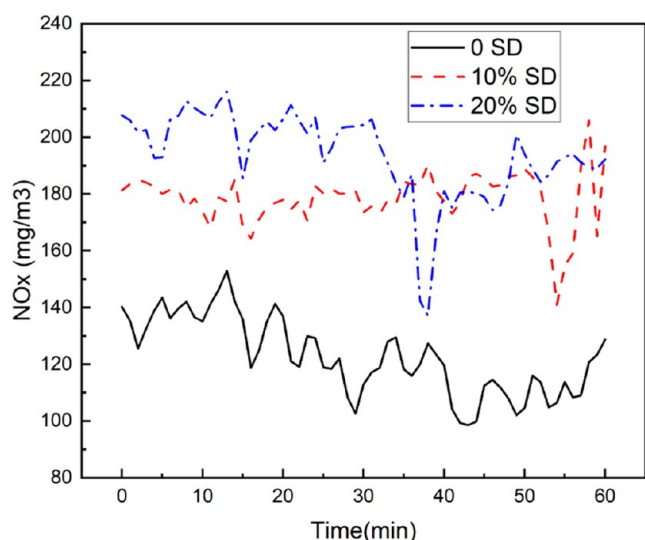


Figure 6. Average furnace temperature under different sludge mixing ratios.

process was characterized by combustion instability, high flue gas volume, and aggravated ash accumulation wear.<sup>32,33</sup> To explore the effect of sludge on furnace combustion, the sludge mixing ratio and load size were adjusted, and the combustion status was monitored after the sludge was mixed. Moreover, in order to investigate the effect of collaborative treatment involving multisource organic solid waste, an experiment was conducted on the combustion of municipal solid waste (MSW), sludge, waste cloth strips, and papermaking waste at different blending ratios. This study provides guidance for



**Figure 7.** NO<sub>x</sub> emissions from combustion with different sludge mixing ratios.

operating and regulating the collaborative disposal of multi-source organic solid waste using municipal solid waste incinerators. The inspection data obtained from the municipal solid waste incineration plant included both industrial and elemental analyses of each material entering the furnace (Table 2).

**4.1. Effect of Sludge Mixing on Furnace Combustion.**  
**4.1.1. Effect of Different Sludge Mixing Ratios on Furnace Combustion.** To ensure a stable operation of the incinerator,

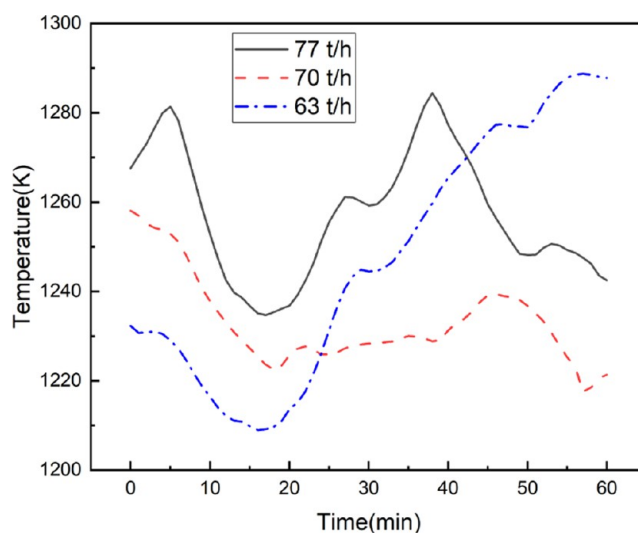


**Figure 9.** Average temperature of furnace combustion mixed with 20% sludge under different loads.

all test conditions were centralized for a specific time, and the incinerator operated under normal conditions for the remaining time. The materials introduced into the furnace were mixed based on mass ratios, and the three groups of test sludge featured mixing ratios of 0, 10, and 20%. With increasing sludge mixing ratio, the temperature level under the field of view of each viewing hole decreased (Figure 5). During the test period, the average furnace temperature decreased from 1240.25 to 1229.85 and 1219.25 K (Figure 6).

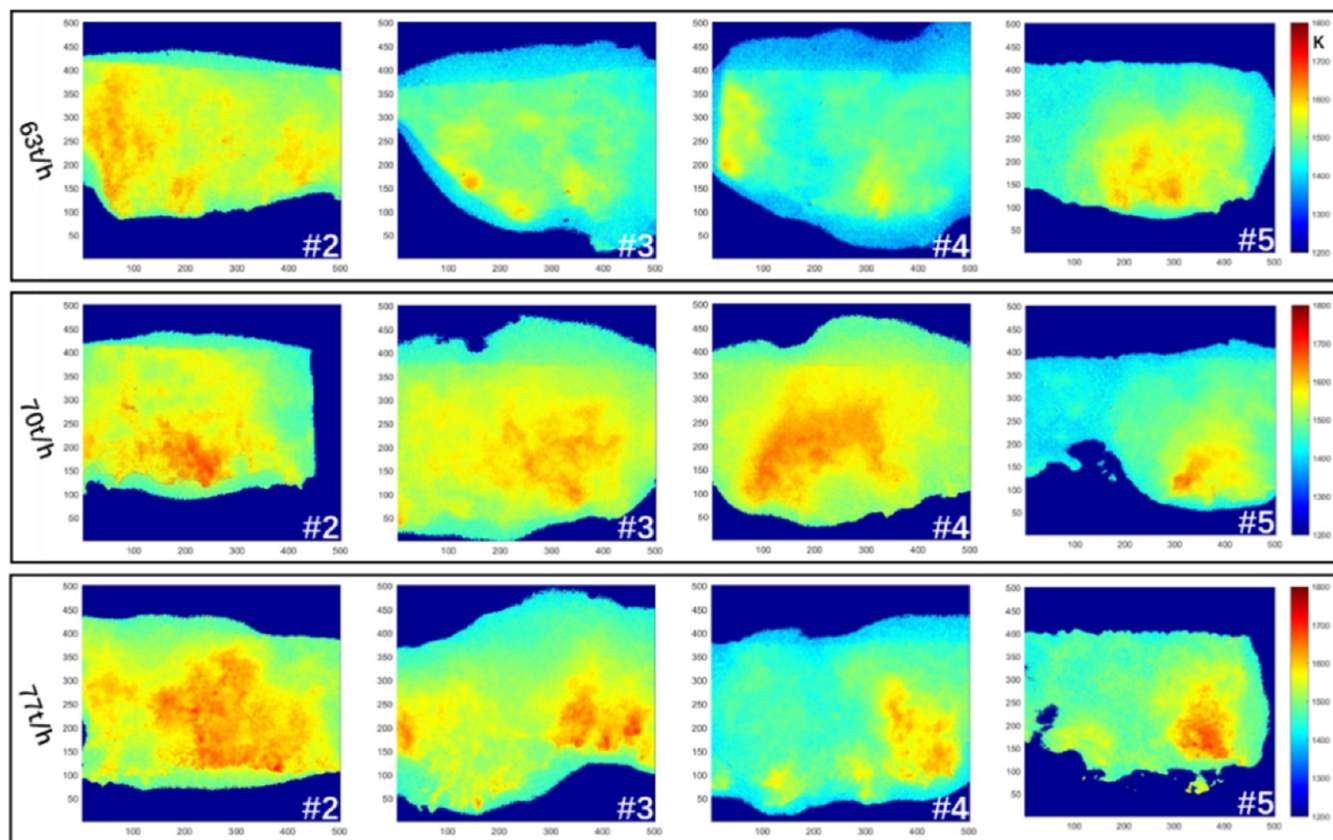


**Figure 8.** Temperature cloud diagram of furnace combustion mixed with 20% sludge under different loads.

Table 3. Multisource Solid Waste Mixing Test

case	test time	experimental content
case 1	2023.3.19 09:00–10:00	MSW: sludge: cloth strips = 8:1:1
case 2	2023.3.19 14:00–15:00	MSW: sludge: cloth strips = 7:1:2
case 3	2023.3.21 09:10–10:10	MSW: sludge: cloth strips: papermaking waste = 7:1:1:1
case 4	2023.3.21 14:00–15:00	MSW: sludge: cloth strips: papermaking waste = 6:1:2:1

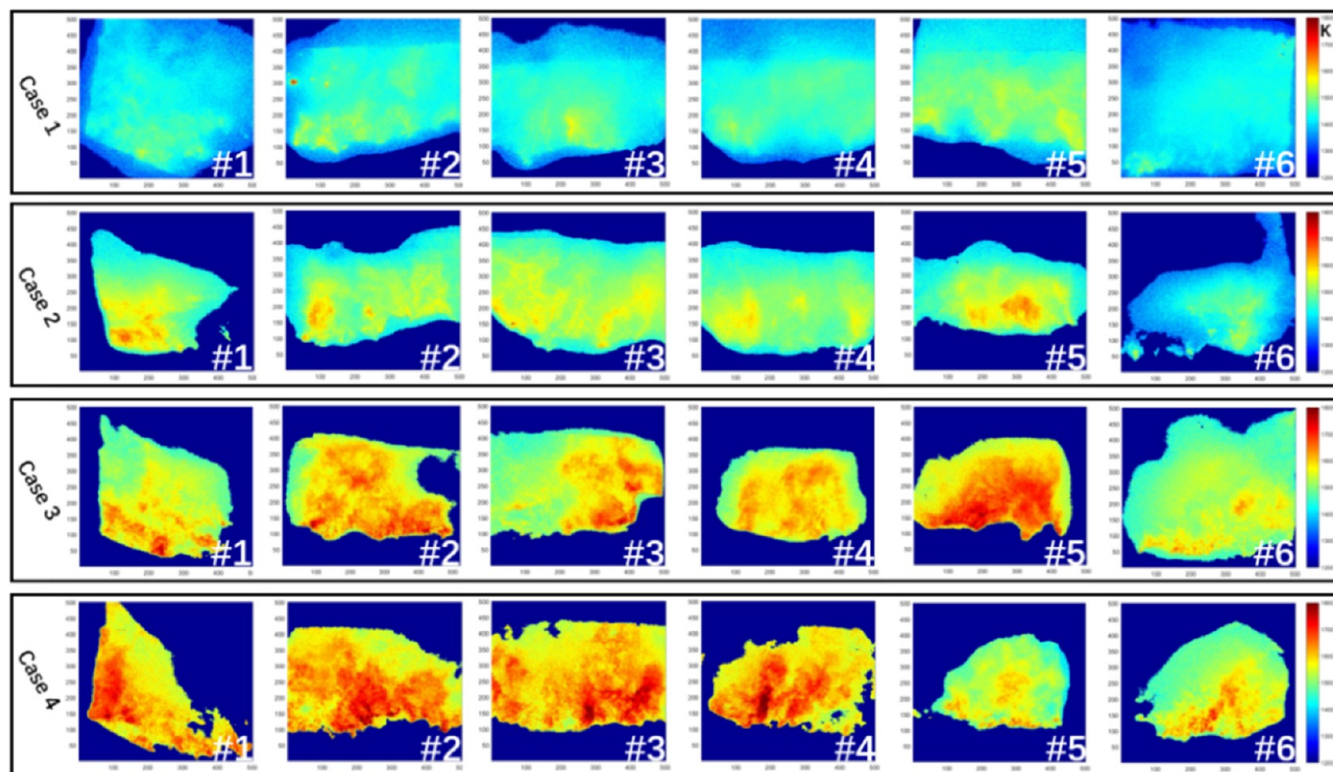


Figure 10. Temperature cloud of combustion with different multisource solid waste mixing ratios.

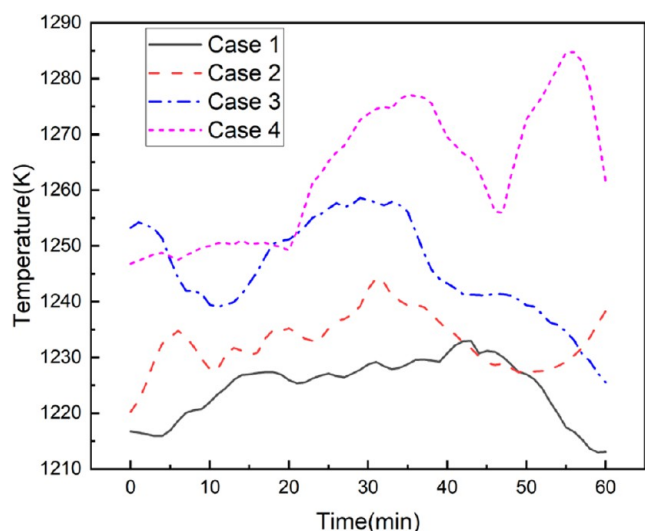


Figure 11. Average furnace temperature for combustion with different multisource solid waste mixing ratios.

Therefore, the overall temperature level inside the furnace slightly decreased as the sludge mixing ratio increased.

As the sludge mixing ratio increased, NO<sub>x</sub> emissions increased (Figure 7). NO<sub>x</sub> was mainly classified into the fuel type, thermal type, and fast type.<sup>34–36</sup> Under the test

conditions, with increasing sludge mixing ratio, the furnace temperature level decreased, and the generation of thermal- and fast-type NO<sub>x</sub> decreased. The municipal solid waste and sludge featured N contents of 2.4 and 6.39%, respectively. After mixing sludge, the N content in the fuel increased, leading to an increase in fuel-type NO<sub>x</sub>.

**4.1.2. Effect of Sludge Mixing on Variable Load Operation.** The load adjustment experiment was performed using the main steam flow as the observation standard. With the rated evaporation capacity of the test boiler at 70 t/h as the benchmark, the test condition was adjusted by  $\pm 10\%$ . Thus, the main steam flow of the load adjustment test was set to 63, 70, and 77 t/h. The temperature level in the furnace was positively correlated with the load, and the overall temperature in the furnace increased as the load increased (Figure 8). The variation in the municipal solid waste calorific value and the municipal solid waste aggregation caused uneven combustion, resulting in localized temperature fluctuations. Moreover, after the load test at 63 t/h was performed, the combustion condition in the furnace deteriorated and the furnace temperature became excessively low (Figure 9), which significantly affected the stable operation of the boiler. To ensure stable operation in the furnace, the load in the central control room was increased. This indicated that the addition of sludge hindered the combustion process in the furnace. This was mainly attributed to the low calorific value and high

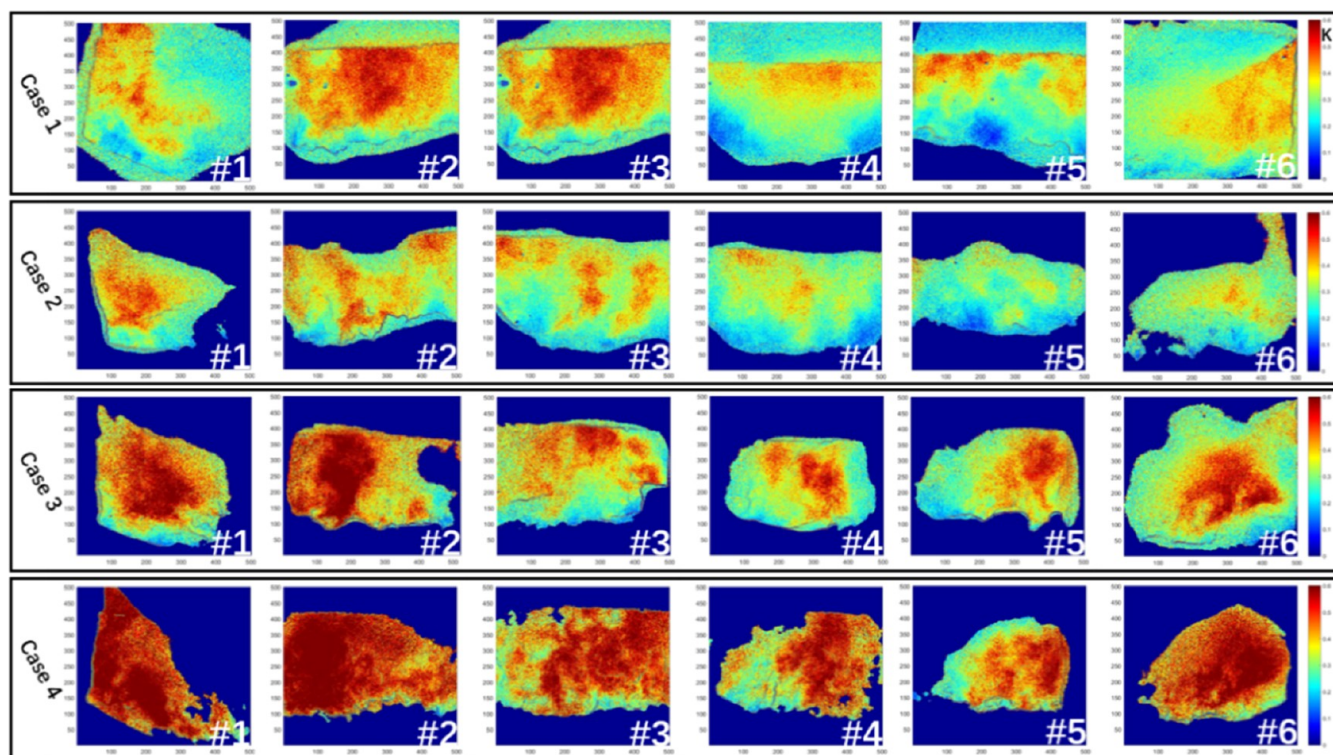


Figure 12. Emissivity cloud of combustion with different multisource solid waste mixing ratios.

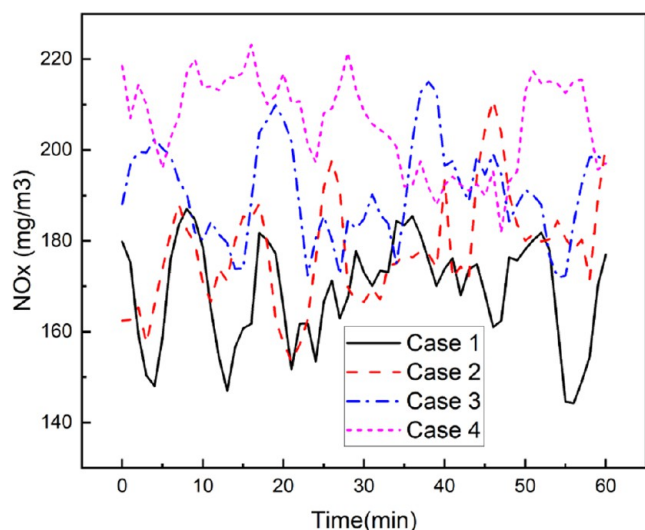


Figure 13. NO<sub>x</sub> emissions from combustion with different multi-source solid waste mixing ratios.

moisture content of the sludge and the large heat consumption for sludge drying during the combustion process, resulting in a decrease in the furnace temperature level.

**4.2. Experimental Exploration of Multisource Organic Solid Waste Mixing.** With the diverse types and properties of organic solid wastes, the effects of various components of organic solid waste on combustion and pollutant emission in the furnace significantly varied. The actual mixing was characterized by increased emission concentration of flue gas pollutants and a poor comprehensive utilization effect. Therefore, experimental research on the collaborative disposal of multisource organic solid waste was conducted to investigate the combustion effect and pollutant emission in the furnace.

This study provides guidance for operating and regulating the actual multisource organic solid waste collaborative disposal. The four sets of working conditions in this test are shown in Table 3.

The analysis of the results from the four sets of tests revealed that during the adjustment process of the mixing ratio (Figure 10), the temperature level for Cases 1 and 2 increased with increasing mixing ratio of cloth strips. Additionally, this temperature increase was observed in the field of view of each flame-viewing hole. In case 3, the addition of papermaking waste led to an increase in the temperature level under the field of view of each flame-viewing holes. In case 4, with increasing mixing ratio of cloth strips, the temperature level under the field of view of each flame-viewing holes further increased. Consequently, the overall temperature level in the furnace gradually increased (Figure 11). The cloth strips and papermaking waste exhibited high calorific values, and the temperature level in the furnace increased during the actual mixing process.

The waste cloth strips exhibited a higher calorific value than that of the papermaking waste, while the overall temperature level of the furnace in case 3 was higher than that of case 2 (Table 2). According to the on-site material conditions, the waste cloth strips tended to entangle and agglomerate, while papermaking waste was relatively broken and scattered. Therefore, during the actual combustion process, the paper waste burned more completely, leading to more efficient combustion and higher furnace temperatures.

The emissivity distribution under different working conditions was positively correlated with the furnace flame temperature distribution (Figure 12). Thus, the overall emissivity level in the furnace increased with the addition of the waste cloth strips and papermaking waste. Under the same working conditions, significant differences occurred in the

emissivity levels at different positions within the furnace. This reflects the uneven distribution of particulate matter concentration in the furnace, indicating nonuniform material and material layer distributions in the municipal solid waste incinerator.

NO<sub>x</sub> emissions gradually increased from case 1 to case 4 (Figure 13). The waste cloth strips exhibited a N content of 1.26%, which is lower than that of municipal solid waste (Table 2). As the mixing ratio of waste cloth strips increased, the total N content of materials decreased, leading to a reduction in the amount of fuel-type NO<sub>x</sub> generated. However, as the temperature level of the furnace increased, the generation of thermal-type NO<sub>x</sub> increased, leading to an increase in the overall NO<sub>x</sub> generation. The papermaking waste featured a N content of 5.07%, which was higher than that of municipal solid waste. After mixing papermaking waste, the total N content of the material increased, the fuel-type NO<sub>x</sub> generation increased, the temperature level of the furnace increased, and the thermal-type NO<sub>x</sub> generation increased. Consequently, the overall NO<sub>x</sub> generation increased.

## 5. CONCLUSIONS

- (1) With increasing sludge mixing ratio, the average temperature of the furnace decreased and the NO<sub>x</sub> emission increased. Moreover, the addition of sludge affected the stable operation of the furnace under low-load conditions. Before mixing, the sludge should be properly dried and dewatered. To control pollutant emissions and ensure the stable operation of the boiler, the sludge mixing ratio should be maintained within a reasonable range and not excessively high.
- (2) After mixing waste cloth strips and papermaking waste, the temperature level in the furnace increased and NO<sub>x</sub> emissions also increased. Thus, the collaborative disposal of organic solid waste with a high calorific value featured a significant effect on the furnace temperature. Additionally, regarding mixing materials with agglomeration and wrapping characteristics, crushing treatment can be performed or the residence time of materials on the grate can be appropriately increased to ensure their complete combustion.
- (3) The mixing rate of different organic solid wastes was controlled within a reasonable range to prevent issues such as excessive pollutant emissions and unstable incinerator operation caused by excessive mixing rate.

## AUTHOR INFORMATION

### Corresponding Author

Zixue Luo – State Key Laboratory of Coal Combustion, Huazhong University of Science & Technology, Wuhan 430074, China; [orcid.org/0000-0001-7360-2799](https://orcid.org/0000-0001-7360-2799); Email: [luozixue@hust.edu.cn](mailto:luozixue@hust.edu.cn)

### Authors

Xiaohui Zhuo – State Key Laboratory of Coal Combustion, Huazhong University of Science & Technology, Wuhan 430074, China

Mi Li – State Key Laboratory of Coal Combustion, Huazhong University of Science & Technology, Wuhan 430074, China

Qiang Cheng – State Key Laboratory of Coal Combustion, Huazhong University of Science & Technology, Wuhan 430074, China

Complete contact information is available at: <https://pubs.acs.org/10.1021/acsomega.3c08369>

## Notes

The authors declare no competing financial interest.

## ACKNOWLEDGMENTS

The authors would like to thank the National Key Research Development Program of China (No. 2019YFC1904003) for financial assistance.

## REFERENCES

- (1) Wang, X. *Opportunities and Challenges in the Context of Building "Waste-Free Cities"*; Low Carbon World, 2021; Vol. 11, pp 18–19.
- (2) Guo, W.; Xi, B. D.; Huang, C. H.; et al. Solid waste management in China: Policy and driving factors in 2004–2019. *Resour., Conserv. Recycl.* **2021**, *173*, No. 173105727.
- (3) Li, X. Problems and countermeasures in urban household waste classification and treatment in China. *J. Environ. Hyg.* **2022**, *12* (5), 321–325.
- (4) Zhang, L. Y. Solid Waste Treatment Methods and Resource Utilization Status. *Shanxi Chem. Ind.* **2020**, *40* (6), 198–200.
- (5) Zhao, J.; Zhang, X. J.; Hong, Ye.; et al. Current Status of Solid Waste Treatment Methods and Resource Utilization Status. *Yunnan Chem. Technol.* **2023**, *50* (6), 14–16.
- (6) China Association of Environmental Protection Industry Municipal Domestic Waste Disposal Specialized Committee. Overview of Municipal Domestic Waste Disposal Industry Development in 2017. *China Environ. Prot. Ind.* **2017**, No. 4, 9–15.
- (7) Samolada, M.-C.; Zabaniotou, A.-A. Comparative assessment of municipal sewage sludge incineration, gasification and pyrolysis for a sustainable sludge-to-energy management in Greece. *Waste Manage.* **2014**, *34* (2), 411–420.
- (8) Zhou, M. H.; Shen, S. L.; Xu, Y. S.; Zhou, A. N. New Policy and Implementation of Municipal Solid Waste Classification in Shanghai, China. *Int. J. Environ. Res. Public Health* **2019**, *16* (17), 3099.
- (9) Sun, X. R.; Zhang, S.; Li, H. Analysis of the hazards of urban stock of domestic waste and comprehensive solution methods. *Energy Environ.* **2016**, No. 1, 73–74.
- (10) Zhao, X. G.; Jiang, G. W.; Li, A.; et al. Technology, cost, a performance of waste-to-energy incineration industry in China. *Renewable Sustainable Energy Rev.* **2016**, 55115–55130.
- (11) Cheng, H. F.; Hu, Y. A. Municipal solid waste (MSW) as a renewable source of energy: Current and future practices in China. *Bioresour. Technol.* **2010**, *101* (11), 3816–3824.
- (12) Wang, R. P. *Thermal Conversion Mechanism of Combustible Solid Waste and Experimental Study in Controlled Atmosphere*; Zhejiang University, 2015.
- (13) Xu, Y. P.; Huang, L. H.; Cui, F. N. Present Situation of the Application and Development of Municipal Domestic Waste Incineration Technology. *Guangdong Chem. Ind.* **2015**, *42* (12), 140–141.
- (14) Cheng, W.; Ju, A. L. Current Situation and Enlightenment on Incineration Treatment of Domestic Waste in Japan. *Environ. Sanit. Eng.* **2019**, *27* (6), 57–60.
- (15) Zhou, D. *Waste-to-Energy Incineration Grows Rapidly in Europe*; Sino-Global Energy, 2018.
- (16) Jiao, X. J.; Huang, J.; Fei, Y. F. Summary of Business Model, Technical Parameters and Facility Characteristics of Waste Incineration Power Generation in America. *Environ. Sanit. Eng.* **2020**, *28* (4), 61–69.
- (17) National Bureau of Statistics. *China Statistical Yearbook*; China Statistics Press: Beijing, 2022.
- (18) Feng, L. L.; Shi, Z. F.; Zhou, Y. G.; et al. Study on Numerical Simulation of Large-scale Waste Incinerator Grate Furnace Co-incineration with Sludge. *Environ. Sanit. Eng.* **2020**, *28* (3), 32–37.



- (19) Yu, W.; Zhu, J. Experimental and simulation studies on the effect of co-incineration of sludge on the combustion process in waste incinerators. *Renewable Energy Resour.* **2021**, *39* (11), 1435–1440.
- (20) Donatello, S.; Tyrer, M.; Cheeseman, C.-R. EU landfill waste acceptance criteria and EU Hazardous Waste Directive compliance testing of incinerated sewage sludge ash. *Waste Manage.* **2010**, *30* (1), 63–71.
- (21) Lynn, C.-J.; Dhir, R.-K.; Ghataora, G.-S.; West, R. P. Sewage sludge ash characteristics and potential for use in concrete. *Constr. Build. Mater.* **2015**, *98*, 98767–98779.
- (22) Zhang, R. N. Impacts of Co-Burning Sewage Sludge on Ash Formation Characteristics in Incineration Grate Furnace of Municipal Solid Waste. *J. Combust. Sci. Technol.* **2021**, *27* (3), 297–302.
- (23) Chen, Z. C.; Tian, X. D.; Li, J. W.; et al. Physicochemical properties and combustion characteristics of coal gasification fine ash modified by NaOH-HCl hydrothermal treatment. *Fuel* **2023**, *333*, No. 333126592.
- (24) Chen, Z. C.; Tian, X. D.; Hou, J.; et al. Sustainable preparation of high-calorific value and low-N and S energy products through the low-temperature alkali fusion of coal gasification fine ash. *Environ. Res.* **2023**, *236*, No. 236116802.
- (25) Chen, W. *Numerical Simulation of Industrial Sludge Blending and Detection Analysis in a New Incinerator*; Huazhong University of Science and Technology, 2021.
- (26) Wang, W. L. *Mechanism and Experimental Research on Thermal Treatment of Organic Solid Waste*; Zhejiang University, 2022.
- (27) Chen, L. M.; Liao, Y. F.; Ma, X. Q.; Niu, Y. Effect of co-combusted sludge in waste incinerator on heavy metals chemical speciation and environmental risk of horizontal flue ash. *Waste Manage.* **2020**, *102*, 102645–102654.
- (28) Luo, Z. X.; Chen, W.; Wang, Y.; et al. Numerical Simulation of Combustion and Characteristics of Fly Ash and Slag in a “V-type” Waste Incinerator. *Energies* **2021**, *14* (22), 7518.
- (29) Xu, H.; An, P. F.; Song, G. M. Research on Integrated Sludge Disposal and Resource Utilization Technology. *China Resour. Compr. Util.* **2019**, *37* (4), 76–78.
- (30) Dai, J. Y.; Xu, M. Q.; Chen, J. P.; et al. PCDD/F, PAH and heavy metals in the sewage sludge from six wastewater treatment plants in Beijing, China. *Chemosphere* **2007**, *66* (2), 353–361.
- (31) Yang, C.; Meng, X. Z.; Chen, L.; Xia, S. Polybrominated diphenyl ethers in sewage sludge from Shanghai, China: Possible ecological risk applied to agricultural land. *Chemosphere* **2011**, *85* (3), 418–423.
- (32) Zhu, J.; Yu, W. Study on Stratified Combustion Characteristics of Sludge in the Cooperative Incineration of Domestic Waste. *Environ. Sanit. Eng.* **2021**, *29* (2), 46–49.
- (33) Rovira, J.; Mari, M.; Nadal, M.; et al. Use of sewage sludge as secondary fuel in a cement plant: human health risks. *Environ. Int.* **2011**, *37* (1), 105–111.
- (34) He, Y. Z.; Luo, J. H.; Li, Y. G.; et al. Comparison of the Reburning Chemistry in O<sub>2</sub>/N<sub>2</sub>, O<sub>2</sub>/CO<sub>2</sub>, and O<sub>2</sub>/H<sub>2</sub>O Atmospheres. *Energy Fuels* **2017**, *31* (10), 11404–11412.
- (35) Lu, F. *Study and Application of Low NO<sub>x</sub> Combustion Technology in Tangential-Firing Pulverized Coal Boiler*; Shanghai Jiao Tong University, 2009.
- (36) Shu, Y.; Zhang, F.; Wang, H. C.; et al. An experimental study of NO reduction by biomass reburning and the characterization of its pyrolysis gases. *Fuel* **2015**, *139*, 139321–139327.